

# First observation of $\gamma$ rays emitted from excited states south-east of $^{132}\text{Sn}$ : The $\pi g_{9/2}^{-1} \otimes \nu f_{7/2}$ multiplet of $^{132}\text{In}_{83}$

A. Jungclauss,<sup>1</sup> A. Gargano,<sup>2</sup> H. Grawe,<sup>3</sup> J. Taprogge,<sup>1,4,5</sup> S. Nishimura,<sup>5</sup> P. Doornenbal,<sup>5</sup> G. Lorusso,<sup>5,6,7</sup> Y. Shimizu,<sup>5</sup> G. S. Simpson,<sup>8</sup> P.-A. Söderström,<sup>5</sup> T. Sumikama,<sup>9</sup> Z. Y. Xu,<sup>10</sup> H. Baba,<sup>5</sup> F. Browne,<sup>11,5</sup> N. Fukuda,<sup>5</sup> R. Gernhäuser,<sup>12</sup> G. Gey,<sup>8,13,5</sup> N. Inabe,<sup>5</sup> T. Isobe,<sup>5</sup> H. S. Jung,<sup>14,\*</sup> D. Kameda,<sup>5</sup> G. D. Kim,<sup>15</sup> Y.-K. Kim,<sup>15,16</sup> I. Kojouharov,<sup>3</sup> T. Kubo,<sup>5</sup> N. Kurz,<sup>3</sup> Y. K. Kwon,<sup>15</sup> Z. Li,<sup>17</sup> H. Sakurai,<sup>5,10</sup> H. Schaffner,<sup>3</sup> K. Steiger,<sup>12</sup> H. Suzuki,<sup>5</sup> H. Takeda,<sup>5</sup> Zs. Vajta,<sup>18,5</sup> H. Watanabe,<sup>5</sup> J. Wu,<sup>17,5</sup> A. Yagi,<sup>19</sup> K. Yoshinaga,<sup>20</sup> S. Bönig,<sup>21</sup> L. Coraggio,<sup>2</sup> J.-M. Daugas,<sup>22</sup> F. Drouet,<sup>8</sup> A. Gadea,<sup>23</sup> S. Ilieva,<sup>21</sup> N. Itaco,<sup>2,24</sup> T. Kröll,<sup>21</sup> A. Montaner-Pizá,<sup>23</sup> K. Moschner,<sup>25</sup> D. Mücher,<sup>12</sup> H. Nishibata,<sup>19</sup> A. Odahara,<sup>19</sup> R. Orlandi,<sup>26,27</sup> and A. Wendt<sup>25</sup>

<sup>1</sup>*Instituto de Estructura de la Materia, CSIC, E-28006 Madrid, Spain*

<sup>2</sup>*Istituto Nazionale di Fisica Nucleare, Complesso Universitario di Monte S. Angelo, I-80126 Napoli, Italy*

<sup>3</sup>*GSI Helmholtzzentrum für Schwerionenforschung GmbH, 64291 Darmstadt, Germany*

<sup>4</sup>*Departamento de Física Teórica, Universidad Autónoma de Madrid, E-28049 Madrid, Spain*

<sup>5</sup>*RIKEN Nishina Center, RIKEN, 2-1 Hirosawa, Wako-shi, Saitama 351-0198, Japan*

<sup>6</sup>*National Physical Laboratory, NPL, Teddington, Middlesex TW11 0LW, United Kingdom*

<sup>7</sup>*Department of Physics, University of Surrey, Guildford GU2 7XH, United Kingdom*

<sup>8</sup>*LPSC, Université Joseph Fourier Grenoble 1, CNRS/IN2P3, Institut National Polytechnique de Grenoble, F-38026 Grenoble Cedex, France*

<sup>9</sup>*Department of Physics, Tohoku University, Aoba, Sendai, Miyagi 980-8578, Japan*

<sup>10</sup>*Department of Physics, University of Tokyo, Hongo 7-3-1, Bunkyo-ku, 113-0033 Tokyo, Japan*

<sup>11</sup>*School of Computing, Engineering and Mathematics, University of Brighton, Brighton BN2 4JG, United Kingdom*

<sup>12</sup>*Physik Department E12, Technische Universität München, D-85748 Garching, Germany*

<sup>13</sup>*Institut Laue-Langevin, B.P. 156, F-38042 Grenoble Cedex 9, France*

<sup>14</sup>*Department of Physics, Chung-Ang University, Seoul 156-756, Republic of Korea*

<sup>15</sup>*Rare Isotope Science Project, Institute for Basic Science, Daejeon 305-811, Republic of Korea*

<sup>16</sup>*Department of Nuclear Engineering, Hanyang University, Seoul 133-791, Republic of Korea*

<sup>17</sup>*School of Physics and State key Laboratory of Nuclear Physics and Technology, Peking University, Beijing 100871, China*

<sup>18</sup>*MTA Atomki, P.O. Box 51, Debrecen H-4001, Hungary*

<sup>19</sup>*Department of Physics, Osaka University, Machikaneyama-machi 1-1, Osaka 560-0043 Toyonaka, Japan*

<sup>20</sup>*Department of Physics, Faculty of Science and Technology, Tokyo University of Science, 2641 Yamazaki, Noda, Chiba, Japan*

<sup>21</sup>*Institut für Kernphysik, Technische Universität Darmstadt, D-64289 Darmstadt, Germany*

<sup>22</sup>*CEA, DAM, DIF, 91297 Arpajon cedex, France*

<sup>23</sup>*Instituto de Física Corpuscular, CSIC-Univ. of Valencia, E-46980 Paterna, Spain*

<sup>24</sup>*Seconda Università di Napoli, Dipartimento di Matematica e Fisica, 2-81100 Caserta, Italy*

<sup>25</sup>*IKP, University of Cologne, D-50937 Cologne, Germany*

<sup>26</sup>*Instituut voor Kern- en Stralingsfysica, K.U. Leuven, B-3001 Heverlee, Belgium*

<sup>27</sup>*Advanced Science Research Center, Japan Atomic Energy Agency, Tokai, Ibaraki, 319-1195, Japan*

(Received 15 December 2015; published 7 April 2016)

For the first time, the  $\gamma$  decay of excited states has been observed in a nucleus situated in the quadrant south-east of doubly magic  $^{132}\text{Sn}$ , a region in which experimental information so far is limited to ground-state properties. Six  $\gamma$  rays with energies of 50, 86, 103, 227, 357, and 602 keV were observed following the  $\beta$ -delayed neutron emission from  $^{133}\text{Cd}_{85}$ , populated in the projectile fission of a  $^{238}\text{U}$  beam at the Radioactive Isotope Beam Factory at RIKEN within the EURICA project. The new experimental information is compared to the results of a modern realistic shell-model calculation, the first one in this region very far from stability, focusing in particular on the  $\pi 0g_{9/2}^{-1} \otimes \nu 1f_{7/2}$  particle-hole multiplet in  $^{132}\text{In}_{83}$ . In addition, theoretical estimates based on a scaling of the two-body matrix elements for the  $\pi h_{11/2}^{-1} \otimes \nu g_{9/2}$  analog multiplet in  $^{208}\text{Tl}_{127}$ , one major proton and one major neutron shell above, are presented.

DOI: [10.1103/PhysRevC.93.041301](https://doi.org/10.1103/PhysRevC.93.041301)

The region of the chart of nuclides south-east of doubly magic  $^{132}\text{Sn}$ , i.e., the nuclei in proximity of  $^{132}\text{Sn}$  with  $Z < 50$  and  $N > 82$ , is of great relevance to the description of the rapid

neutron capture process of nucleosynthesis, in particular after the break-out from the  $N = 82$  waiting point nuclei. From the nuclear structure point of view, the study of these nuclei, which are the furthest off stability experimentally accessible today, may give important information on the shell evolution and on the underlying driving forces. They actually play a special role within the framework of the shell model, offering

\*Present address: Department of Physics, University of Notre Dame, Notre Dame, Indiana 46556, USA.



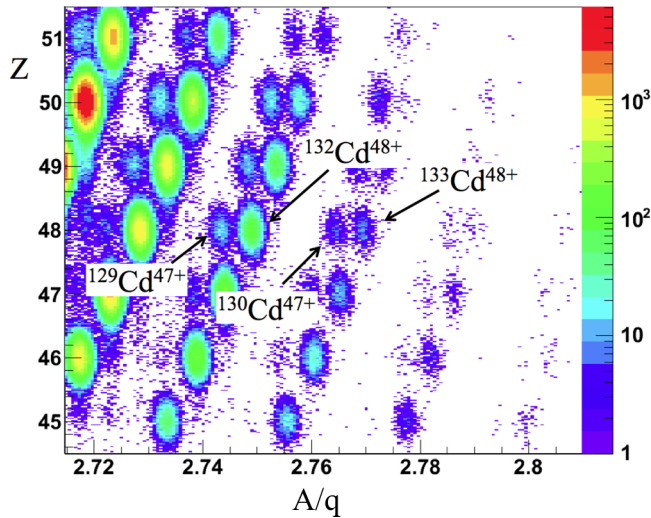


FIG. 2. Partial particle identification plot showing all events according to the reconstructed values of the atomic mass  $Z$  and the mass-to-charge ratio  $A/q$ . Note the clear separation between the fully stripped (i.e.,  $q = Z$ )  $^{132,133}\text{Cd}$  ions and the hydrogen-like  $^{129,130}\text{Cd}$  ions ( $q = Z - 1$ ).

of 100 keV to 7% at 1 MeV. Note that no add-back of signals registered in neighboring Ge crystals has been applied in the present work.

In Ref. [1] a  $\log ft$  value of 5.4 was estimated for the first-forbidden decay  $\nu 1f_{7/2} \rightarrow \pi 0g_{9/2}$  from the  $0^+$  ground state of  $^{132}\text{Cd}$  (with configuration  $\pi g_{9/2}^{-2} \otimes \nu f_{7/2}^2$ ) to the  $1^-$  member of the  $\pi g_{9/2}^{-1} \otimes \nu f_{7/2}$  multiplet in  $^{132}\text{In}$ , the only significant decay branch populating excited states in  $^{132}\text{In}$  below the neutron separation energy ( $P_n = 60\% \pm 15\%$  [1]). For this  $\log ft$  value the  $1^-$  state is expected to be populated in 20–30% of all  $^{132}\text{Cd}$  decays. Consequently, taking into account the 8600 observed decays and the  $\gamma$  efficiencies quoted above, a few hundred counts are expected for the  $\gamma$  transitions connecting this  $1^-$  state to the  $7^-$  ground state. However, as discussed in Ref. [20], no distinct  $\gamma$  rays were observed in the energy range below 900 keV in prompt coincidence with the decay of  $^{132}\text{Cd}$  ions implanted into WAS3ABi, possibly indicating a larger  $\beta$ -delayed neutron emission probability as reported in the literature. In contrast, a number of low-energy  $\gamma$  rays are observed following the 640 recorded decays of  $^{133}\text{Cd}$  ions. Since a “ $P_n$  value close to 100%” was reported for  $^{133}\text{Cd}$  in Ref. [3], these  $\gamma$  rays are assumed to be emitted from excited states in  $^{132}\text{In}$ .

Figure 3(a) shows the spectrum of  $\gamma$  rays observed in prompt coincidence with  $\beta$ -decay events registered within the first 200 ms after the implantation of an identified  $^{133}\text{Cd}$  ion into WAS3ABi. Five lines at energies of 50, 103, 227, 357, and 602 keV are clearly visible in this spectrum and there are indications for at least one additional line in the range between 50 and 100 keV. In order to reduce the low-energy background in this spectrum, we considered in the next step only those events in which only one of the seven crystals in a Ge cluster detector registered an energy deposition. This condition, which

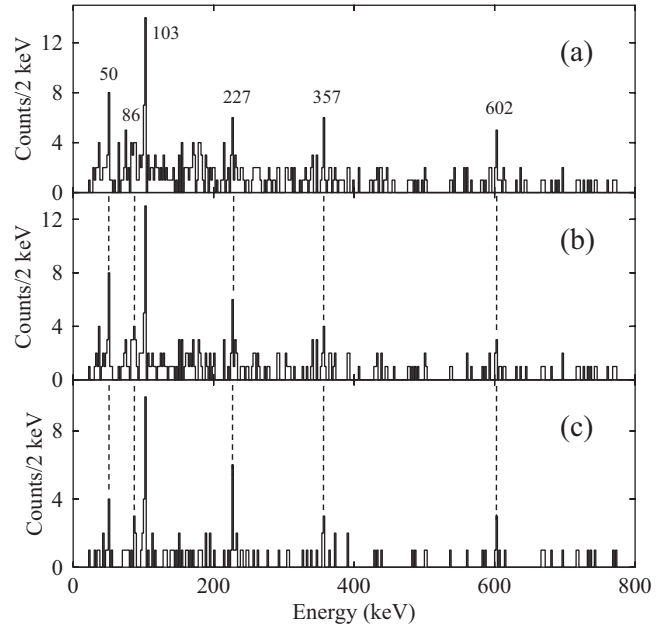


FIG. 3.  $\gamma$ -ray spectra in prompt coincidence with decay events during the first 200 ms after the implantation of a  $^{133}\text{Cd}$  ion into WAS3ABi. (a) Without further condition, (b) requiring multiplicity one in the composite Ge detector, and (c) applying in addition a strict spatial correlation discussed in detail in the text.

favors photopeak events over signals belonging to Compton scattered  $\gamma$  rays, resulted in the  $\gamma$ -ray spectrum shown in Fig. 3(b). To further clean up the spectrum a very strict spatial correlation between the implantation and the decay is required. Figure 3(c) is obtained when only those events are considered in which the decay took place either in the Si detector in which the ion was implanted or in the one in front or behind. Furthermore, in the plane perpendicular to the beam axis, the decay had to occur within 1 mm of the implantation position in both the vertical and the horizontal directions. The background is now significantly reduced as compared to Fig. 3(a), in particular in the low-energy region. In addition to the five lines listed above there is now clear evidence of the existence of a sixth line at an energy of 86 keV. The statistics accumulated in the present experiment are very limited (see Fig. 3) so that unfortunately no conclusive  $\gamma\gamma$  coincidence information could be obtained.

To compare these six observed  $\gamma$  rays with theoretical predictions, a realistic effective interaction was derived for the first time for nuclei in the quadrant south-east of  $^{132}\text{Sn}$ . We take  $^{132}\text{Sn}$  as closed core and consider a model space spanned by the four  $0f_{5/2}$ ,  $1p_{3/2}$ ,  $1p_{1/2}$ ,  $0g_{9/2}$  proton-hole orbitals and the six  $1f_{7/2}$ ,  $2p_{3/2}$ ,  $2p_{1/2}$ ,  $0h_{9/2}$ ,  $1f_{5/2}$ ,  $0i_{13/2}$  neutron orbitals. The adopted values of the neutron single-particle and proton single-hole energies are taken from the experimental spectra of  $^{133}\text{Sn}$  [21,22] and  $^{131}\text{In}$  [20], respectively, except those of the  $\nu 0i_{13/2}$  and the  $\pi 0f_{5/2}^{-1}$  orbitals, whose corresponding states have not yet been observed. The energies of these two orbitals are from Refs. [23] and [20], respectively. The two-body effective interaction is derived within the framework of the  $\hat{Q}$ -box folded diagram expansion [24] starting from the

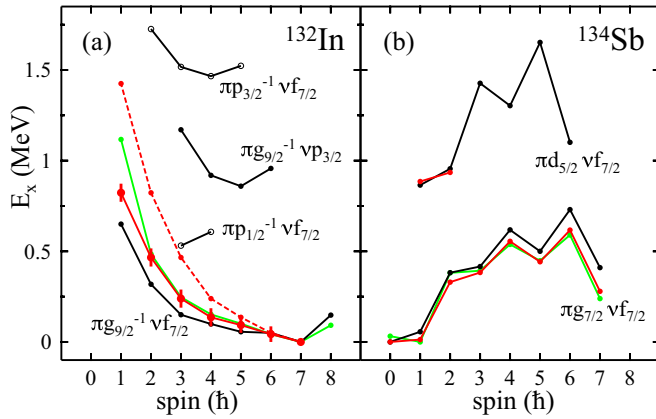


FIG. 4. Lowest particle-hole and, respectively, particle-particle multiplets in (a)  $^{132}\text{In}$  and (b)  $^{134}\text{Sb}$ . Filled circles correspond to negative-parity and open circles to positive-parity states. Results of SM calculations using realistic effective interactions are shown in black (for  $^{134}\text{Sb}$  from Ref. [28]), while SM estimates based on a scaling of TBMEs from the  $^{208}\text{Pb}$  region are given in green. Experimentally proposed states are represented by red dots (for  $^{134}\text{Sb}$  from Ref. [29]). For  $^{132}\text{In}$ , the dashed red line represents the level energies obtained assuming that the six  $\gamma$  rays observed in the present experiment form a cascade from the  $1^-$  state to the  $7^-$  ground state while the full red line results from the assumption that one low-energy transition escaped observation (see text for details).

high-precision CD-Bonn  $NN$  potential [25], renormalized by means of the  $V_{\text{low}-k}$  approach [24] with a cutoff momentum  $\Lambda = 2.2 \text{ fm}^{-1}$ . The  $\hat{Q}$  box is obtained by including diagrams up to second order in  $V_{\text{low}-k}$ , which are computed within the harmonic-oscillator basis with  $\hbar\omega = 7.88 \text{ MeV}$ . It is worth pointing out that the neutron-proton effective interaction has been explicitly derived in the particle-hole formalism as described in Ref. [26]. All calculations are performed with the OXBASH shell-model code [27]. The four multiplets calculated at lowest excitation energy in the proton-hole, neutron-particle nucleus  $^{132}\text{In}$  are shown in Fig. 4(a). As expected, the members of the  $\pi g_{9/2}^{-1} \otimes \nu f_{7/2}$  multiplet form the negative-parity yrast sequence while the  $\pi p_{1/2}^{-1} \otimes \nu f_{7/2}$  configuration at energies slightly above 500 keV is the lowest positive-parity one. The second excited  $3^-$ – $6^-$  states, belonging to the  $\pi g_{9/2}^{-1} \otimes \nu p_{3/2}$  configuration, are positioned about 0.75–1.0 MeV above the yrast line. Finally, the  $\pi p_{3/2}^{-1} \otimes \nu f_{7/2}$  multiplet is predicted at excitation energies around 1.5 MeV.

For a start, we assume in the following that the six observed  $\gamma$  rays correspond to the expected cascade of  $M1$  transitions from the  $1^-$  member of the  $\pi g_{9/2}^{-1} \otimes \nu f_{7/2}$  multiplet down to the  $7^-$  ground state. This assumption is based on the observation made in several experimental studies [29–32] that, due to the  $E^5$  dependence of  $\beta$  decay,  $\beta$ -delayed neutron emission tends to populate states at low excitation energy in the daughter nucleus. For example, in the decay of the  $(7/2^-)$  ground state of  $^{135}\text{Sn}$  via neutron emission to excited states in  $^{134}\text{Sb}$  [29], a case which is very similar to the one discussed here with respect to the relative excitation energies of different configurations in the daughter nucleus as shown in Fig. 4(b), primarily the members of the  $\pi g_{7/2} \otimes \nu f_{7/2}$

multiplet are populated. The  $1^-$  and  $2^-$  states with excitation energies around 900 keV, which belong to the  $\pi d_{5/2} \otimes \nu f_{7/2}$  configuration, receive at most 6% of the total feeding [29]. The resulting excitation energies, assuming that all six observed transitions connect states of the  $\pi g_{9/2}^{-1} \otimes \nu f_{7/2}$  multiplet and ordering them according to their energies, are compared to the results of the SM calculations in Fig. 4(a). In this scenario, the experimental energies are systematically higher than the calculated ones, leading to a total energy spread which is twice as large as theoretically predicted. The average difference between experimental and calculated excitation energies is  $\approx 300 \text{ keV}$ , which corresponds to roughly 50% of the SM energy spread.

Realistic SM calculations using the same approach as described above have been reported in the past for a number of proton-particle, neutron-hole multiplets, namely, the  $\pi g_{9/2} \otimes \nu g_{9/2}^{-1}$ , the  $\pi g_{7/2} \otimes \nu d_{3/2}^{-1}$  and the  $\pi h_{9/2} \otimes \nu f_{5/2}^{-1}$  states in  $^{90}\text{Nb}_{49}$ ,  $^{132}\text{Sb}_{81}$ , and  $^{208}\text{Bi}_{125}$  [26,33–35], respectively, and also for the particle-particle nuclei  $^{210}\text{Bi}$  [36] and  $^{134}\text{Sb}$  [28]. For  $^{134}\text{Sb}$ , the results of SM calculations are included in Fig. 4(b). These calculations very nicely reproduce the shape of the spread in energy, and also agree with experiment for the excitation energies of the  $1^-$  and  $2^-$  members of the  $\pi d_{5/2} \otimes \nu f_{7/2}$  configuration. In all the cases listed above, the agreement is of comparable quality and the average difference between experimental and calculated level energies amounts to less than 10% of the SM energy spread of the respective multiplet. In view of this consistently obtained good agreement between experiment and SM calculations for a significant number of cases, the comparison shown in Fig. 4(a) seems to disprove our original assumption that the six observed  $\gamma$  transitions form a single cascade. From the experimental side it can of course not be excluded that one or more low-energy transitions escaped observation. For example, the calculated energy for the  $5^- \rightarrow 6^-$  transition is only 6 keV. Assuming that one of the lowest transitions within the multiplet is unobserved and adopting an energy of  $25 \pm 25 \text{ keV}$  for this transition, excitation energy ranges can be estimated for all states of the multiplet as shown in Fig. 4(a). Note that in this scenario the 602 keV  $\gamma$  ray would correspond to the decay of a higher lying excited state, belonging to either the  $\pi p_{1/2}^{-1} \otimes \nu f_{7/2}$  or the  $\pi g_{9/2}^{-1} \otimes \nu p_{3/2}$  multiplet. The resulting excitation energies are now much closer to the SM predictions and the average difference drops to 80 keV, i.e., 12% of the SM energy spread, comparable to that found in all other cases studied so far. It therefore seems likely that one of the low-energy transitions within the multiplet indeed escaped observation.

Besides the realistic SM calculations discussed above there is an alternative theoretical approach to studying nuclei with only a few nucleons or holes outside the doubly magic  $^{132}\text{Sn}$  core. It is based on the known similarities between the nuclear structure properties of nuclei in the  $^{132}\text{Sn}$  and  $^{208}\text{Pb}$  regions [37,38]. As was recognized already more than 30 years ago by Blomqvist [37], every proton or neutron single-particle state in the  $^{132}\text{Sn}$  region with quantum numbers  $(n, l, j)$  has its analog state in the  $^{208}\text{Pb}$  region, one harmonic oscillator shell higher, with quantum numbers  $(n, l + 1, j + 1)$ .



Furthermore, the matrix elements of the effective interactions in the  $^{132}\text{Sn}$  and  $^{208}\text{Pb}$  regions are expected to be proportional to each other. In several studies [29,39,40] unknown two-body matrix elements in the  $^{132}\text{Sn}$  region were derived from the interaction designed by Warburton for nuclei in the  $^{208}\text{Pb}$  region [41]. In all these cases, using the prescription given in Ref. [37], the interaction strengths were scaled up by a factor of  $(208/132)^{1/3}$  corresponding to the mass dependence of a finite-range interaction in an oscillator basis. Here, we followed the same procedure to calculate the states belonging to the  $\pi g_{9/2}^{-1} \otimes \nu f_{7/2}$  configuration in  $^{132}\text{In}$  from the TBME for the  $\pi h_{11/2}^{-1} \otimes \nu g_{9/2}$  multiplet in  $^{208}\text{Tl}$  [41]. Note that no configuration mixing was considered. The resulting energies are shown in green in Fig. 4(a). As for the realistic SM interaction, a much better agreement with experiment is obtained assuming that one low-energy transition escaped observation. In this case the multiplet is perfectly reproduced by the theory in the spin range 2–7, only the  $1^{-}$  state is predicted too high in energy (about 300 keV). Note that the estimate obtained in the same way for the  $\pi g_{7/2} \otimes \nu f_{7/2}$  multiplet in  $^{134}\text{Sb}$ , inferred from the TBME for the  $\pi h_{9/2} \otimes \nu g_{9/2}$  configuration in  $^{210}\text{Bi}$ , yields excellent agreement with experiment as shown in Fig. 4(b). In contrast to the particle-particle multiplet in  $^{134}\text{Sb}$ , the  $\pi g_{9/2}^{-1} \otimes \nu f_{7/2}$  hole-particle configuration in  $^{132}\text{In}$  exhibits negligible odd-even staggering which supports the chosen  $\gamma$ -ray sequence in descending order.

To summarize the above discussion: Assuming that the six  $\gamma$  rays observed following  $\beta$ -delayed neutron emission from  $^{133}\text{Cd}$  in the present work form a cascade of  $M1$  transitions between the members of the multiplet expected to be lowest in  $^{132}\text{In}$ , namely, the  $\pi g_{9/2}^{-1} \otimes \nu f_{7/2}$  configuration, the experimental  $1^{-}-7^{-}$  energy spread is strongly underestimated by both the SM calculation employing a modern realistic effective interaction and the estimate based on a  $A^{-1/3}$  mass scaling of TBME designed for nuclei in the  $^{208}\text{Pb}$  region. On the other hand, considering the possibility that one of the low-energy transitions within the  $\pi g_{9/2}^{-1} \otimes \nu f_{7/2}$  multiplet escaped observation, a much better agreement between the experimental excitation energies and the two different theoretical approaches is obtained. More precisely, the quality of the results obtained from the realistic SM calculation is in this case of the same order as found for several other particle-hole and particle-particle multiplets in different mass regions.

In conclusion, in the present work we reported on the very first observation of  $\gamma$  decays from excited states of a nucleus situated in the quadrant south-east of  $^{132}\text{Sn}$ , namely, its one proton-hole, one neutron neighbor  $^{132}\text{In}$ . On the theoretical side, we presented the first shell-model calculation considering neutrons in the  $N = 82-126$  and proton holes in the  $Z = 28-50$  major shells. The TBME were derived from the  $NN$  potential within the framework of the many-body theory. The comparison between experiment and theory suggests that at least four of the six observed transitions connect members of the  $\pi g_{9/2}^{-1} \otimes \nu f_{7/2}$  multiplet, while at least one more likely corresponds to the decay of an excited state belonging to another configuration. The present work constitutes an important first step toward the exploration of the nuclear structure in a region of the nuclear chart, which, although crucial for nucleosynthesis processes, is presently still a terra incognita as far as excited state properties are concerned. With the steadily increasing beam intensities provided by radioactive ion beam facilities around the world it is to be expected that more comprehensive experimental information, for  $^{132}\text{In}$  as well as other nuclei in the region, will soon become available. This will allow one to ascertain the capability of different nuclear models to provide reliable predictions for physical quantities in regions of the isotope chart which will remain inaccessible for experimental studies.

We thank the staff of the RIKEN Nishina Center accelerator complex for providing stable beams with high intensities to the experiment. We acknowledge the EUROBALL Owners Committee for the loan of germanium detectors and the PreSpec Collaboration for the readout electronics of the cluster detectors. This work was supported by the Spanish Ministerio de Ciencia e Innovación under Contract No. FPA2011-29854-C04 and the Spanish Ministerio de Economía y Competitividad under Contract No. FPA2014-57196-C5-4-P, the Generalitat Valenciana (Spain) under Grant No. PROMETEO/2010/101, the National Research Foundation of Korea (NRF) grant funded by the Korea government (MEST) (No. NRF-2012R1A1A1041763), the Priority Centers Research Program in Korea (2009-0093817), OTKA Contract No. K-100835, JSPS KAKENHI (Grant No. 25247045), the European Commission through the Marie Curie Actions call FP7-PEOPLE-2011-IEF under Contract No. 300096 and the German BMBF (No. 05P12RDCIA and No. 05P12RDNUP), and Helmholtz International Center for FAIR.

- 
- [1] M. Hannawald *et al.* (ISOLDE Collaboration), *Phys. Rev. C* **62**, 054301 (2000).  
 [2] I. Dillmann *et al.*, *Eur. Phys. J. A* **13**, 281 (2002).  
 [3] K.-L. Kratz, B. Pfeiffer, O. Arndt, S. Hennrich, A. Wöhr, and the ISOLDE/IS333, IS378, IS393 Collaborations, *Eur. Phys. J. A* **25**, 633 (2005).  
 [4] G. Lorusso *et al.*, *Phys. Rev. Lett.* **114**, 192501 (2015).  
 [5] D. Atanasov *et al.*, *Phys. Rev. Lett.* **115**, 232501 (2015).  
 [6] G. S. Simpson *et al.*, *Phys. Rev. Lett.* **113**, 132502 (2014).  
 [7] A. Jungclaus *et al.*, *Phys. Rev. Lett.* **99**, 132501 (2007).  
 [8] H. Watanabe *et al.*, *Phys. Rev. Lett.* **111**, 152501 (2013).  
 [9] L. Coraggio, A. Covello, A. Gargano, N. Itaco, and T. T. S. Kuo, *Phys. Rev. C* **80**, 044320 (2009).  
 [10] L. Coraggio, A. Covello, A. Gargano, and N. Itaco, *Phys. Rev. C* **81**, 064303 (2010).  
 [11] L. Coraggio, A. Covello, A. Gargano, and N. Itaco, *Phys. Rev. C* **87**, 034309 (2013).  
 [12] L. Coraggio, A. Covello, A. Gargano, and N. Itaco, *Phys. Rev. C* **89**, 024319 (2014).  
 [13] B. Fogelberg, M. Hellström, D. Jerrestam, H. Mach, J. Blomqvist, A. Kerek, L. O. Norlin, and J. P. Omtvedt, *Phys. Rev. Lett.* **73**, 2413 (1994).

- [14] T. Kubo *et al.*, Prog. Theor. Exp. Phys., 03C003 (2012).
- [15] N. Fukuda, T. Kubo, T. Ohnishi, N. Inabe, H. Takeda, D. Kameda, and H. Suzuki, Nucl. Instrum. Meth. B **317**, 323 (2013).
- [16] S. Nishimura *et al.*, Prog. Theor. Exp. Phys., 03C006 (2012); RIKEN Accel. Progr. Rep. **46**, 182 (2013).
- [17] P.-A. Söderström *et al.*, Nucl. Instrum. Methods B **317**, 649 (2013).
- [18] J. Eberth, H. G. Thomas, P. v. Brentano, R. M. Lieder, H. M. Jäger, H. Kämmerling, M. Berst, D. Gutknecht, and R. Henck, Nucl. Instrum. Methods Phys. Res., Sect. A **369**, 135 (1996).
- [19] J. Simpson, Z. Phys. A **358**, 139 (1997).
- [20] J. Taprogge *et al.*, Phys. Rev. Lett. **112**, 132501 (2014).
- [21] P. Hoff *et al.*, Phys. Rev. Lett. **77**, 1020 (1996).
- [22] K. L. Jones *et al.*, Nature **465**, 454 (2010).
- [23] L. Coraggio, A. Covello, A. Gargano, and N. Itaco, Phys. Rev. C **65**, 051306(R) (2002).
- [24] L. Coraggio, A. Covello, A. Gargano, N. Itaco, and T. T. S. Kuo, Prog. Part. Nucl. Phys. **62**, 135 (2009), and references therein.
- [25] R. Machleidt, Phys. Rev. C **63**, 024001 (2001).
- [26] L. Coraggio, A. Covello, A. Gargano, N. Itaco, and T. T. S. Kuo, Phys. Rev. C **66**, 064311 (2002).
- [27] B. A. Brown, A. Etchegoyen, and W. D. M. Rae, the Computer Code OXBASH, MSU-NSCL Report No. 524 (unpublished).
- [28] L. Coraggio, A. Covello, A. Gargano, and N. Itaco, Phys. Rev. C **73**, 031302(R) (2006).
- [29] J. Shergur *et al.*, Phys. Rev. C **71**, 064321 (2005).
- [30] A. Korgul *et al.*, Phys. Rev. C **86**, 024307 (2012).
- [31] A. Korgul *et al.*, Phys. Rev. C **88**, 044330 (2013).
- [32] K. Miernik *et al.*, Phys. Rev. C **88**, 014309 (2013).
- [33] L. Coraggio, A. Covello, A. Gargano, and N. Itaco, Phys. Rev. C **85**, 034335 (2012).
- [34] K. H. Maier *et al.*, Phys. Rev. C **76**, 064304 (2007).
- [35] A. Covello, L. Coraggio, A. Gargano, and N. Itaco, Phys. At. Nucl. **67**, 1611 (2004).
- [36] L. Coraggio, A. Covello, A. Gargano, and N. Itaco, Phys. Rev. C **76**, 061303(R) (2007).
- [37] J. Blomqvist, CERN Report No. 81-09, CERN, Geneva, 1981 (unpublished), p. 535.
- [38] L. Coraggio, A. Covello, A. Gargano, and N. Itaco, Phys. Rev. C **80**, 021305(R) (2009).
- [39] A. Korgul *et al.*, Eur. Phys. J. A **15**, 181 (2002).
- [40] M. Gorska *et al.*, Phys. Lett. B **672**, 313 (2009).
- [41] E. K. Warburton, Phys. Rev. C **44**, 233 (1991).